Thermoeconomic analysis of a biogas upgrading process in solid oxide electrolysis cells (SOEC)

Guido Lorenzi[a], Andrea Lanzini[b], Massimo Santarelli[b], Carlos A. Santos Silva[a]
[a] IN+, Instituto Superior Técnico, Universidade de Lisboa, Avenida Rovisco Pais 1, 1049-001, Lisbon, Portugal. guido.lorenzi@tecnico.ulisboa.pt
[b] Department of Energy, Politecnico di Torino, Corso Duca degli Abruzzi 24, 10129, Torino, Italy.

Abstract:
A promising route to fulfill the target fixed by the European Commission of 10% share of biofuels in the transport sector by 2020 is represented by upgrading biogas to biomethane. Biogas as such cannot easily be used in car engines because of its low energy density, so the methane content needs to be increased above 90% vol.. The aim of this paper is to assess a process for biogas upgrading by means of a high temperature electrolysis process based on solid oxide electrolysis cells (SOEC) that exploit the co-electrolysis of CO_2 and H_2O. The obtained syngas is injected in a cascade of methanator reactors to increase the heating value of biogas and to make it suitable for conventional natural gas end-use technologies. The main strength of biogas upgrading via electrolysis lies in its higher synthetic natural gas productivity for given raw digester gas feed at the only expense of the electricity required to run the electrolysis process that should be ideally sourced from a low-carbon source (e.g., surplus electricity from intermittent renewable power sources). Exergy and thermo-economic analysis can be applied to the co-electrolytic upgrading process to assess the weight of the installation costs and of the inefficiencies, due to the design of the process, on the total cost of the final product.

Keywords:
Power-to-gas, digester gas, synthetic natural gas, SOEC, electrolysis

1. Introduction

The target on 10% share of renewable energies in the transportation sector that the European Commission has set for 2020 (Directive 2009/28/EC) is promoting the research and the implementation of processes for biomass transformation into fuels. In particular, anaerobic digestion (AD) for digester gas production has become a diffuse way of transforming waste biomass into energy products [1]. Biological substrate sources may include agricultural residues, manure, sewage sludge, the organic fraction of municipal solid waste and energy crops. Biomass can basically be divided into wet and dry types, according to the initial water content. Dry biomass (water content <50% wt.) can be treated through flash pyrolysis or subdued to further drying before being burned [2]. Digester gas from the anaerobic digestion of sludge from a waste-water treatment plant is considered in the present work. For this kind of wet biomass anaerobic digestion is the most appropriate conversion process [3]. An upgrade plant should ideally be located in a waste-water treatment plant or landfill, where digester gas from urban sewage or municipal solid wastes can be simply obtained.

The main components of raw digester gas are methane, carbon dioxide and water. Its energy density, which is quite low compared to other gaseous fuels, depends on the methane fraction and varies between 16 and 23 MJ/Nm^3, according to the nature of the substrate. Its use in boilers or engines can therefore be problematic or inconvenient. For this reason, it is advisable to upgrade this gas in order to meet the requirements prescribed for natural gas grid injection. After transformation, the final gas product (generally called SNG – Synthetic Natural Gas) usually contains 95-97% vol. CH_4 and 1-3% vol. CO_2 [4]. However, digester gas upgrading has recently become part of a larger research topic, namely power-to-gas, which considers the use of nuclear or renewable surplus electricity to produce synthetic fuels through electrolysis. The interaction between the two contexts is remarkable because power-to-gas pathways need carbon (unless only hydrogen is produced), which can be retrieved by refining digester gas, whose production is increasing in Europe thanks to the introduction of dedicated subsidies.

In this framework, the different methods for CO_2 dissociation and conversion into synthetic fuels, involving high temperature electrolysis devices (e.g., SOEC) are mainly set up as twofold processes. Their first stage consists of the injection of water and purified biogas or CO_2 as feed streams for an SOEC stack; water is reduced into hydrogen and carbon dioxide is reduced into carbon monoxide. Methanation reactors, placed downstream from the SOEC, then transform hydrogen and carbon monoxide into methane. An already available commercial catalytic process that can be used to obtain this result is named TREMP™ ("Topsøe Recycle Energy-efficient Methanation Process"[5]). This process allows the calorific value of the gaseous mixture to be raised by increasing its methane content to very high molar fractions (>90% vol.).
The possibility of coupling power-to-gas with a digester gas upgrade process can be considered in this context. With this technique the input gas can be electrolyzed to yield a syngas rich in H_2 and CO, using the feeding CO_2 as the carbon source, and then transform it into synthetic methane.
During the digester gas to synthetic natural gas upgrade process through an SOEC, the presence of a nickel based catalysts in the fuel electrodes favours the steam reforming of methane. An Ni catalyst, in fact, not only promotes electrochemical reactions, but also the catalytic decomposition of methane through steam reforming ($\mathbf{CH_4 + H_2O \rightarrow 3H_2 + CO}$). Since this reaction is endothermic, it helps avoid methane consumption inside the SOEC in order to prevent additional heat from being supplied to the stack. This heat is generally released through the irreversible operation of the SOEC (i.e., polarization effects). Consequently, the electricity supplied to the SOEC is partially wasted as irreversible heat, which contributes to the maintenance of a constant operating temperature. When digester gas obtained from proteinaceous feedstocks is considered, sulfide compounds are mostly found as contaminants in the form of hydrogen sulfide (H_2S), and range from 0.005 to 2% vol. It is well known that sulfur poisons nickel catalysts, even though it reduces the catalytic activity of the steam reforming reaction to a greater extent than the catalytic activity that promotes the electrochemical reactions [6]. Therefore, the concentration of H_2S should be a trade-off between the effects of the two competing phenomena (chemical and electrochemical reactions). In addition, the system should contain a sulfur removing device in order to eliminate all the traces of H_2S from the SOEC outlet stream, in order to avoid poisoning of the methanator catalysts.
The diffusion of this route for digester gas upgrading depends on its economic feasibility, which is affected by the conditions of natural gas and electricity markets. The purpose of this work is to perform a thermoeconomic (also called exergoeconomic) analysis of the digester gas upgrading process proposed and patented by J. B. Hansen [7], in order to characterized the process of cost formation of the final product, i.e. synthetic natural gas.

2. Plant dynamic behaviour

The proposed concept is more suitable for continuous operation, due to the limited flexibility of the catalytic methanation unit and to the possible accelerated degradation of the SOEC from thermo-mechanical stress generated by a supply that can vary to a great extent. Although renewable energy sources are the ideal power supply, they are intermittent and difficult to predict. A possible alternative would be to use nuclear power to cover the demand. A second solution could foresee the presence of a syngas storage unit. According to this scenario, the SOEC operates in 'supply-following' mode and the generated syngas is compressed and temporarily stored in tanks in order to allow continuous operation of the downstream methanation synthesis section.
The dynamic capability of the SOEC has already been demonstrated at the single-cell and stack levels [8], but not at a system level. In case of the temporarily absence of surplus renewable electricity, the SOEC could even be maintained at open circuit voltage (OCV), i.e., in hot stand-by conditions, for several hours, without any significant thermal losses [9], as the stack units are surrounded by a thick insulation layer.

3. Process layout

The digester gas upgrading system comprises three main sections: pressurization and heating of the reactants, electrolysis and methanation (Figure 1). The assumptions on the mechanical and electrical performance coefficients of the pressure changer devices are provided in Table 1.

Table 1: Components' efficiencies used for the calculation of the electric power

η_{is} compressors	0.8
η_{is} pumps	0.8
η_{el} compressors	0.95
η_{el} pumps	0.9
η_{AC-DC} rectifier[1]	0.98

The electrolysis process was assumed to take place in a commercial cathode supported SOEC and the methanation process involves three adiabatic methanators with a commercially available mixed Ni non-Ni catalyst, thanks to which it is possible to reach low temperatures at the inlets of the methanators.

The modeled plant is fed with liquid water and with a gaseous mixture of methane and carbon dioxide, which represents digester gas. The latter is assumed to have an average molar composition of 60% CH_4 and 40% CO_2 on a vol. basis, with a controlled H_2S partial pressure. All the reactants are assumed available at atmospheric pressure and 20 °C. The feed streams have to be conditioned to be suitable for SOEC operation. The SOEC inlet temperature is set to 800 °C, while the electrolytic reactions are considered to take place at 850°C. The temperature increase from 800 °C to 850 °C is accomplished inside the stack by exploiting additional heat generation due to polarization effects. The configuration in which the surplus heat is used to heat up the reactants is named the "*extended thermoneutral*" configuration. In other words, the irreversible phenomena that occur within the SOEC supply all the heat required for the electrolytic reactions (as would happen in the case of the classical thermoneutral condition [6]) and for the final heating of the reactants.

Table 2: Pressure loss for the plant's components

Component	**Pressure loss [bar]**
HE2 + HE5 + HE4 (cold side)	1.2
HE1, HE3, HE6 (cold side)	0.7
SOEC	1
COOLERS	0.5
HE1+HE2 (hot side)	0.7
DESULFURATOR	1
METHANATORS	0.5

The SOEC is modeled as isothermal, and the stack is run in extended thermoneutral conditions with fixed current. Since there is a direct correlation between the SOEC reactant flows and the input current, the mass flow to be pre-heated can be determined.

Therefore, the size of the plant (and thus the syngas production) depends on the total Faradic current[2] absorbed by the SOEC module, which has here been set to 100,000 A. Consequently, the main output of the design process is the value of the active area of the cells. This represents the size of the installation and it constitutes a considerable share of the investment cost of the whole plant. Once the flow has been electrolyzed, it is passed through a desulfurization unit in order to remove all the traces of sulfur, thus preventing the catalyst in the downstream methanation section from being poisoned. The only effect of the desulfurization process on the thermodynamic conditions of the stream is a pressure loss. The methanation process consists of three steps, each of which involves an adiabatic Gibbs type reactor and a cooler. CO and H_2 are converted into methane through methanation and water gas shift reactions, respectively. The reaction heat produces a considerable increase in temperature and recycling is therefore used to control the temperature rise in the first methanation reactor (outlet temperature below 600 °C). The inlet reactor temperature was set at 220 °C. The gas then enters the subsequent methanation stages. The feed stream of the first methanator is subjected to a composition constraint ($\frac{[H_2]-[CO_2]}{[CO]+[CO_2]} = 3$, expressed in terms of partial pressures). When the molar amount of CH_4 is sufficiently high, water is separated through condensation. The water can be used cleverly by injecting it upstream from the SOEC stack, before pumping, in order to minimize the consumption of the demineralized water. Finally, a gas rich in methane is obtained, whose quality can be adjusted in order to meet the grid specifications. Aspen

[1] The power to the stack is withdrawn from the grid and supplied in the form of direct current, therefore the AC-DC conversion efficiency needs to be accounted.

[2] The Faradic current is the current absorbed by an electrolytic machine to perform the dissociation of the reactants.

Plus® chemical process design software is used to calculate the performance of all the plant components, whose pressure drops are indicated in Table 2.

Figure 1: Scheme of the plant

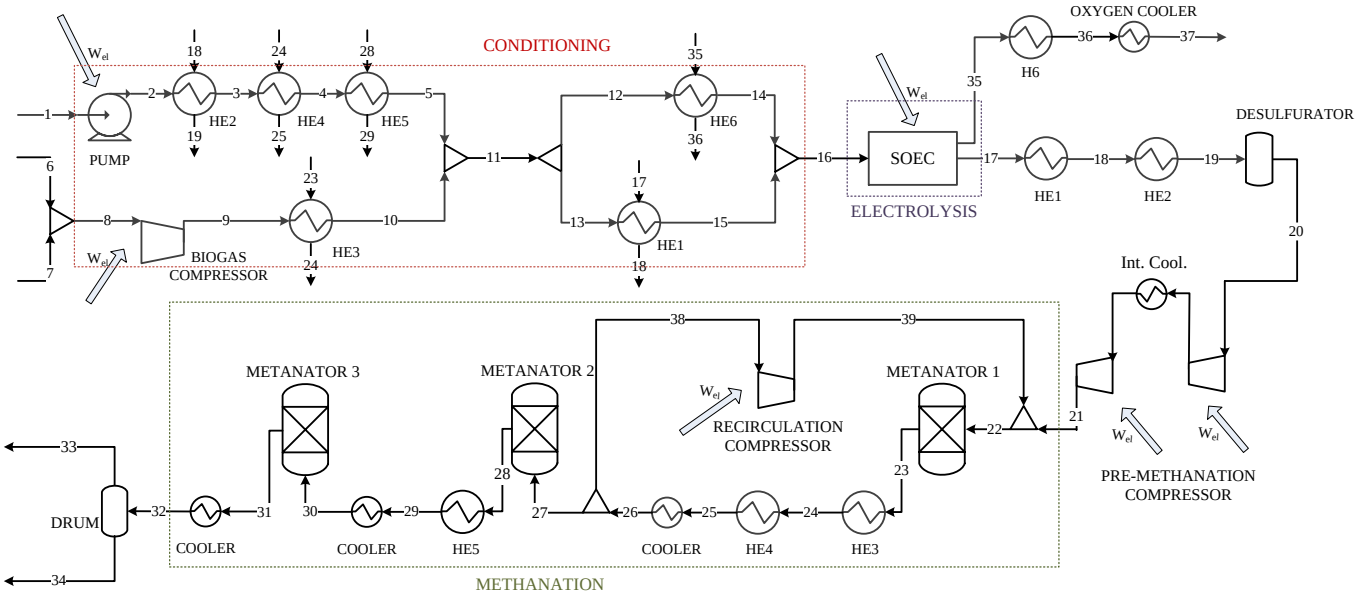

4. Energy analysis results

The conditions in which the performance of the plant was assessed are summarized in Table 3. Since the inlet pressure in the first methanator was set to 33 bar and the stack of cells is run close to atmospheric pressure, a syngas compressor was required downstream from the SOEC reactor to feed the methanator section. The efficiency of the plant was calculated according to (1)[3]:

$$\eta_{pl} = \frac{LHV_{SNG} * \dot{m}_{SNGout}}{LHV_{CH_4}\dot{m}_{CH_{4in}} + W_{el,pl}} \qquad (1)$$

The thermal integration of the plant has been calculated and its thermal self-sufficiency has been proved as explained in detail in section 5. The result in terms of energy efficiency is quite high and this can be mainly ascribed to two factors: firstly, the higher efficiency of the SOEC compared with other electrolysis cells [10]; secondly, the necessary heat to bring the reactants to the stack inlet conditions is provided by the cooling down of the products of the electrolyzer and of the downstream methanators.

The system is affected by a performance drop due to the presence of sulfur[4] in the inlet biogas and it implies an increase in the overall resistance of the cells. This quantity is usually expressed through a parameter called Area Specific Resistance (ASR). Therefore, a lower current density is sufficient to maintain thermoneutral operation. Nevertheless, this fact implies an increase in the active area that is necessary to produce the constant Faradic current value. In Table 4 it is possible to see that around 85% of the total inlet power is necessary for the electrolysis reactions, so it is the part of the plant where the design should be more accurate in order to limit the losses. The first law efficiency of the SOEC stack (η_I^{SOEC}) in thermoneutral conditions is expressed by $\eta_I^{SOEC} = \frac{\Delta H}{W_{el}^{SOEC}}$ and in this case is equal to 0.98. It is a very high value because the losses are due only to the conversion form AC (grid power) to DC current, as required for the electrolysis.

Table 3: Operating parameters for the SOEC plant

SOEC operating temperature	[°C]	850
SOEC operating pressure	[bar]	~1
First methanator inlet pressure	[bar]	33

[3] LHV_{SNG} = Lower Heating Value of the SNG; LHV_{CH_4} = Lower Heating Value of methane; $\dot{m}_{SNGout}$ = SNG outlet mass flow; $\dot{m}_{CH_{4in}}$ = methane inlet mass flow; $W_{el,pl}$ = electric power demand of one-step upgrading plant, kW.

[4] Sulfur is necessary to prevent the steam reforming reaction from occurring in the SOEC, but it entails also a reduction of the electro catalytic efficiency [6].

Faradic current	[A]	100000
Thermoneutral Voltage, V_{TN}	[V]	1.33
Ideal (or Gibbs) Voltage, VG	[V]	0.94
Current density, j	[A/cm^2]	0.57
Active area of the cells, A	[cm^2]	175346
Area specific resistance, ASR	[Ω*cm^2]	0.69
Power density	[W/cm^2]	0.75

Table 4: Mass and energy flows of the plant

Total AC electric need	[kW]	161.51
Pumping Power	[kW]	23.98
Stack Power	[kW]	137.53
Upgraded Gas (SNG)	[kg/h]	18.88
Methane inlet	[kg/h]	11.19
Methane chemical energy flow	[kW]	155.54
LHV_{SNG}	[MJ/kg]	49.45
SNG chemical energy flow	[kW]	259.26
Efficiency	[%]	82

5. Thermal integration of the plant

Under the thermal perspective the process can be mainly divided into two sections: upstream and downstream from the SOEC. In the former it is necessary to supply heat to the streams in order to bring them to the conditions required by the stack operation. Instead, in the latter it is necessary to remove heat in order to reach the desired operating conditions for components like compressors and methanators. Therefore, it is possible to use the heat produced by the second half of the process in order to satisfy the thermal needs of the first section. The coupling can be done through the pinch analysis methodology [11].

Pinch analysis is used to design networks of heat exchangers for energy systems. The constraints which have to be satisfied are usually the extreme temperatures of the fluids involved in the process, inasmuch they cannot be changed without compromising the operation of the sub-processes. The targets that are used to orientate the design of the network of heat exchangers can include the minimization of the external heat requirement or the minimization of the total heat exchange area (which is proportional to the heat exchanger cost). The most important design parameter to be specified is the minimum temperature difference (ΔT_{PP}) between the hot fluids (i.e. those which have to be cooled down) and the cold ones (i.e. those which have to be heated up). This quantity affects both the minimum energy requirement and the heat exchange area. In the present work the value of $\Delta T_{PP} = 20^oC$ has been chosen, which is generally adopted for the chemical plants.

A list of the heat exchangers, with correspondent hot and cold fluids, is given in Table 5, while the composite curves are reported in Figure 2. In this plot, the curve of the cold fluids was shifted to the right by a quantity equal to the total external thermal need (-32 kW).

The excess heat is more than one third of the total heat produced. If it is assumed that there are no other thermal needs outside the plant (e.g. district heating networks or bottoming cycles) the design of the network of the heat exchanger should also focus on restraining the number of the heat exchanger and, in turn, the total heat exchange area.

The network obtained after the match of the hot resources with the cold demands can be seen in Figure 1, where for every heat exchanger the inlet and outlet streams are reported. In Table 5 a more detailed description of the feature of the heat exchanger is provided.

It is possible to prove that in this particular case the minimum number of heat exchanger is equal to the sum of the hot flows, the cold ones and the external resources minus one. In this case the minimum number of heat exchanger is 10, as those that have been designed.

In order to compose the network, it was necessary to split the inlet stream of the SOEC in order to exploit efficiently the heat of the anode and cathode outlet streams. Instead, for the design of others heat exchangers (i.e. used to heat the reactants before their mixing) the choice was to couple streams with a high temperature difference to minimize the exchange area. This carries a benefit in terms of investment cost, even though the rate of exergy destruction is higher.

Figure 2: Composite curves for cold and hot flows

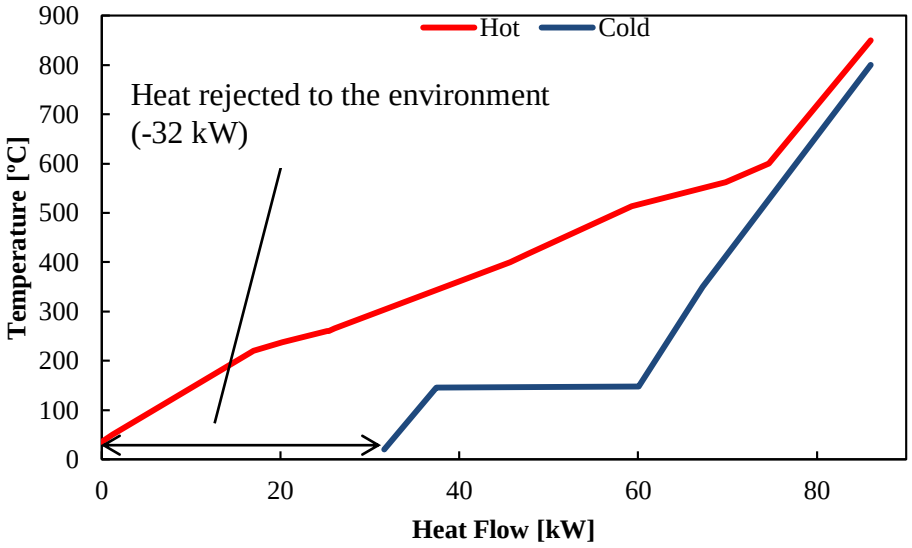

Table 5: Summary of the heat exchangers.

Heat exchanger	Side	Tin [°C]	Tout [°C]	Thermal flow [W]	G*cp [W/K]	Area [m2]
HE1	hot	850	418	15784	36.5	2.70
	cold	350	800		35.1	
HE2	hot	418	237	5836	32.3	0.24
	cold	20	145		46.7	
HE3	hot	600	562	3124	82.7	0.10
	cold	143	350		15.1	
HE4	hot	400	260	4114	29.3	0.54
	cold	148	350		20.4	
HE5	hot	562	265	22541	76.0	0.95
	cold	145	148		7178.5	
HE6	hot	850	514	3006	8.9	0.31
	cold	350	800		6.7	
Cooler 1	hot	265	220	3124	68.7	0.29
	cold	20	40		156.2	
Cooler 2	hot	260	220	1103	27.7	0.11
	cold	20	40		55.1	
Cooler 3	hot	514	50	3788	8.2	0.47
	cold	20	40		189.4	
Cooler 4	hot	261	35	19001	84.3	4.97
	cold	20	40		950.1	

6. Exergy analysis results

The energy analysis showed that the plant has a considerably high first law efficiency. Therefore, the assessment of the plant exergy flows is useful to confirm the good energy performance of the plant as renewable storage facility. In particular, a detailed analysis of the exergy content of each flow was conducted. Since the process includes several chemical reactors, it was necessary to account both for the physical and the chemical exergy associated to each stream.

The exergy computation has been made referring all the streams to the dead state conditions [13]. Instead, the reference state for enthalpy and entropy is described in [12].

The physical exergy (b_f) has been calculated as in (2):

$$b_f - b_{fo} = (h - h_0) - T_0 \times (s - s_0) \qquad (2)$$

Instead, the chemical exergy (b_{ch}) was computed with the formula (3), in which R is the universal gas constant (8.314 J/mol/K) and $b_{ch,i}$ is the molar chemical exergy of a substance in the dead state [13]:

$$b_{ch} = \sum_i y_i \, b_{ch,i} + RT_0 \sum_i y_i \times \ln(y_i) \qquad (3)$$

For the sake of brevity only the exergy content for the plant inlet and outlet energy and mass streams are reported in Table 6. The negative values of physical exergy are due to the choice of the dead state.

Table 6: Exergy performance of the plant. The inlet flows are in red, the outlet ones in blue.

Mass/Energy Stream ID	Physical exergy, Ψ_{ph} [kJ/kg]	Chemical exergy, Ψ_{ch} [kJ/kg]	Total specific exergy, ψ [kJ/kg]	Total exergy, Ψ [kW]
1	1.87E-01	5.18E+01	5.20E+01	5.29E-01
6	-1.96E+00	5.18E+04	5.18E+04	1.61E+02
7	-6.61E-01	4.52E+02	4.51E+02	2.57E+00
33	5.13E+02	5.12E+04	5.17E+04	2.71E+02
34	4.15E+00	5.14E+01	5.56E+01	3.03E-01
37	5.35E+01	1.25E+02	1.79E+02	1.48E+00
Wel pump	-	-	-	7.85E-03
Wel biogas compressor	-	-	-	2.02E+00
Wel SOEC	-	-	-	1.38E+02
Wel methanation compressor	-	-	-	2.18E+01
Wel recirculation compressor	-	-	-	1.93E-01
Total inlet exergy [kW]				**325**
Total outlet exergy [kW]				**272**
η_{ex} [%]				**83**

6.1 Exergetic costs

The exergetic cost of a flow is the amount of exergy that must be spent, in the upstream transformations, for the obtainment of the exergy of the flow itself. In other words, it is a measure of the exergy necessary to attribute to a generic flow its exergy content.

Considering the exergy balance of a generic component ($\Psi_{\text{in}} = \Psi_{out} + \Psi_D$), the exergy cost of the outlet flow is defined as: $\Psi^*_{out} = \Psi_{\text{in}} > \Psi_{\text{out}}$. By explicating the exergetic cost balance ($\Psi^*_{out} - \Psi^*_{in} = 0$), it is easy to notice that the exergetic cost is, unlike exergy, a conservative quantity.

Consequently, it is possible to define the concept of unit exergetic cost of an exergy flow as: $k^* = \frac{\Psi^*}{\Psi} \geq 1$.

Considering a system composed by *n* components and *m* flows, the exergetic cost balance could be written as:

$$\sum_{j=1}^{m} a_{ij}\Psi^*_j = 0 \quad \forall\, i = 1, \dots, n$$

Where: $a_{ij} = 1$ if the j[th] flow enters the i[th] component; $a_{ij} = -1$ if the j[th] flow exits the i[th] component; $a_{ij} = 0$ if the j[th] flow is not connected to the i[th] component.

The same balance can be expressed in matrix form by the introduction of the incidence matrix **A** $[n\ x\ m]$, containing the parameters a_{ij} with the defined signs, which represents the topological description of the system. The exergetic cost balance can be, thus written as: $\boldsymbol{A} \cdot \overline{\Psi^*} = \bar{0}$.

The number of flows *n* is usually higher than the number of components *m* and some additional equations have to be added to solve the system. They are written in the form $\bar{\alpha} \cdot \overline{\Psi^*} = \omega$ and they can be determined according to the following rules:

1. the exergetic cost of the k[th] flow coming from the external environment is equal to the exergy content of the flow itself ($\alpha_k = 1; \omega = \Psi_k$);
2. if in a component, the fuel is defined as the difference between the exergy contents of the outlet k[th] and of the inlet flow (k-1)[th], the two flows assume the same unit exergetic cost ($\alpha_k = -\frac{\Psi_{k-1}}{\Psi_k};\ \alpha_{k-1} = 1; \omega = 0$);
3. if a component has a total product composed by more than 1 exergy flows, they assume the same unit exergetic cost ($\alpha_k = -\frac{\Psi_{k-1}}{\Psi_k};\ \alpha_{k-1} = 1; \omega = 0$);

The complete list of the exergetic costs and unit exergetic costs is reported in Table 10. As expected the sum of the exergetic costs of the outlet flows (33, 34 and 37) equates the inlet total exergy. Furthermore, the inverse of the unit exergetic cost can be interpreted as the exergetic efficiency to produce the considered exergy flow. Thence, by applying this to the outlet streams it is possible to compute the exergetic efficiency for each product. For the considered plant the values are: $\eta_{ex}^{SNG} = \eta_{ex}^{H_2O\ DEMI} = 0.84$ and $\eta_{ex}^{OXYG} = 0.41$. In the present case, since the exergy content of the SNG is enoursmously higher than that of the other outlet flows, the overall plat efficiency is very close to

η_{ex}^{SNG}, but this is not always the case. In fact, thermoeconomic analysis is very useful to discriminate which product has the less efficient production line in a multiproduct process.

6.2 Performance indices

In order to assess the exergy performance of the process, some indices have been introduced and their value for all the components are reported in Table 7:

- Relative Irreversibility $\chi_i = \frac{\Psi_{D,i}}{\Psi_{D,tot}}$ - it is the irreversibility flow produced in the ith component $\Psi_{D,i}$, referred to the total irreversibility produced in the whole plant $\Psi_{D,tot}$.
- Exergetic Factor $f_i = \frac{\Psi_{F,i}}{\Psi_{F,tot}}$ - the parameter expresses the fraction of the fuel elaborated by the single ith component $\Psi_{F,i}$ over the fuel exergy flow elaborated by the whole plant $\Psi_{F,tot}$. It is the amount of the total exergy resources of a system used by a single component. It can be proved that the highest effect on the exergy efficiency of a system is due to components which have low value of exergy efficiency (η_{ex}) and high consumption of exergy resources, thus high exergetic factor f. Therefore, to maximize the exergy efficiency of the whole systems, it is better to focus on the improvement of components with high exergetic factors. From Table 7 it is possible to notice that all the components that release heat to the environment have a zero η_{ex} because the cooling of a stream above the ambient temperature is equivalent to a loss. Then, the economizer (HE2) and the evaporator (HE4) have quite low efficiencies because they are designed with high temperature difference to limit the exchange area. This solution was adopted since there are no different use of the available heat, that would, however, be released to the environment. The intercooled compressor has an efficiency that is lower than the other two compressors because the heat between the two compression stages is not recovered. The SOEC has very high second law efficiency and it means that the electrical energy used to feed it is not degraded very much. This is ascribable to the high temperature of the product gases are available to the electrolysis of H_2O and CO_2 into substances with a high chemical exergy content. The SOEC, the pre-methanation compressor, the cooler 4 and the oxygen cooler are the components which destroy the biggest quantity of the fuel exergy. In the SOEC the transformation of electrical exergy into chemical and thermal exergy (considered in the reactants' temperature increase) is characterized by irreversible processes. In the other components the losses are mainly due to the release of heat flows with a considerable exergy contents, because of the lack of additional heat demand.

Table 7: Indices of exergetic performance for the plant.

Component	Exergy efficiency, η_{ex} [%]	Rate of exergy destroyed, Ψ_D [W]	Exergetic factor, f	Relative irreversibility, χ
PUMP	72.00%	2	0.00%	0%
HE2	27.59%	2374	1.01%	4%
HE4	49.98%	6333	3.89%	12%
HE5	82.98%	357	0.64%	1%
BIOGAS COMPRESSOR	76.00%	485	0.62%	1%
HE3	57.57%	889	0.64%	2%
HE1	90.75%	1002	3.33%	2%
HE6	90.93%	186	0.63%	0%
SOEC	90.43%	13165	42.22%	24%
OXYGEN COOLER (COOLER 3)	0.00%	3310	1.02%	6%
DESULFURATOR	0.00%	1530	0.47%	3%
PRE-METHANATION COMPRESSOR	53.76%	10060	6.68%	19%
METHANATOR 1	99.55%	3124	213.29%[5]	6%
RECIRCULATION COMPRESSOR	76.00%	46	0.06%	0%
COOLER 1	0.00%	1347	0.41%	3%
METHANATOR 2	99.56%	1229	86.51%	2%
COOLER 2	0.00%	499	0.15%	1%
METHANATOR 3	99.89%	315	85.34%	1%
COOLER 4	0.00%	4895	1.50%	9%
DRUM	99.61%	1069	83.74%	2%

7. Economic analysis

The second step for a thermo-economic evaluation of the plant is the definition of the costs of the exergy flows entering the system and the costs for the installation and maintenance of the plant.
Since the purpose of this work is to apply the methodology to a case study, some strong assumptions have been made in order to simplify the procedure.
In particular, only to the main components of the plants have been attributed a cost for the purchase of the equipment. The costs of the other components, of the piping and of labour have been included in the operation and maintenance (O&M) factor.
The assumptions and the sources of information are summarized in Table 8 and Table 9.

Table 8: Cost estimation for the main components of the plant

Component	Methodology	Reference
Compressor	Correlation for rotary compressor in carbon steel	[14]
High Temperature Heat Exchangers (T>500°C)	Correlation for double pipe heat exchangers in Ni-alloy	[14]
Medium Temperature Heat Exchangers (T<500°C)	Correlation for double pipe heat exchangers in carbon steel	[14]
Methanators	Downscale of the value found in the reference proportional to the lower SNG mass flow rate, since a similar composition of the flowing gas is assumed	[15]

Table 9: Economic assumptions for two different scenarios

Parameter	Case A	Case B
Capacity factor, CF	0.5	0.85
O&M (fraction of the equipment cost per year)	10%	10%
Capital recovery factor, CRF	0.163	12%
Interest Rate, i	10%	10%
Plant Lifetime [yr], l_t	10	20
Demineralized water price [$/m3]	2.3	2.3
Digester gas price[16] [c$/kWh]	1.4	1.4
Natural gas price [c$/kWh]	2.14	2.14
Electricity price [c$/kWh]	6.44	0

8. Thermo-economic analysis

[5] This value is greater than 1 because the components are part of a recirculation loop and, hence, some exergy is recycled and does not come from the external environment.

Thermoeconomics is an engineering field which originates from the integration of the laws of thermodynamics and economic variables. This discipline was born mainly to provide objective and thermodynamically correct criterion for the determination of the costs in a multiproduct system. In our approach for thermo-economic analysis is intended a rigorous method that evaluates the *exergoeconomic* performances of processes and plants.
The thermoeconomic analysis combines together the first and second law of thermodynamics with cost balances evaluated at the component level. Such methodological approach helps understand the cost formation process within the power plant and provides a tool to identify and eventually minimize the overall plant product cost (e.g., SNG) [17].
The plant has been defined before as a set of units linked to each other and to the environment by a set of matters, heat and work flows. The relation between flows and subsystems is set up through the incident matrix $\mathbf{A}$ $[n\ x\ m]$ described in section 6.1. The more detailed is the definition of the incidence matrix, the higher are the chances to identify the causes of inefficiency. Valero et al. [18] formulated a rational procedure for determining costs, based on five main propositions:
1. The equations of exergetic cost balance are equal to the number of units in the installation;
2. An equation for each flow entering the system has to be formulated, specifying its cost;
3. Without external assessment, the cost value of a stream leaving the plant control volume is set to zero.
In case of multiple outlet flows, *m-n* additional equations must be written. Their determination of can be done with the following propositions:
4. If the resource of a component is defined as the difference of two flows, then the same unit exergetic cost will be assigned to all of them.
5. If a unit has a product composed of several flows, then the same unit exergetic cost will be assigned to all of them.
The thermoeconomic cost balance for any single unit of the plant can be expressed[6] as:

$$\Pi_F + Z = \Pi_P$$

And the final system of equations to be solved takes the form $\mathbf{A} \times \overline{\Pi} = \overline{Z}$, where matrix dimensions are: $[m\ x\ m] \times [m\ x\ 1] = [m\ x\ 1]$.
To evaluate the thermoeconomic performance, the cost of exergy destruction and the exergoeconomic factor were calculated for every component. The cost of exergy destruction (C_D) is the cost of the fuel entering the unit (c_F), multiplied by the rate of exergy destroyed (Ψ_D):

$$C_D = c_F \cdot \Psi_D$$

The exergoeconomic factor (f_{ex}) is defined as the total capital cost over to the sum of total capital cost and the cost of exergy destruction within a certain component:

$$f_{ex} = \frac{Z}{(C_D + Z)}$$

9. Results and discussion

The thermoeconomic analysis was applied to the SOEC plant considered in this study. The costs of inlet resources are the digester gas, the electricity and the demineralized water prices reported in Table 9. Looking at Table 10, the thermoeconomic cost increases its value through every component since each component adds its capital investment and O&M cost. The cost of the stream 33 is the production cost of the SNG expressed in $/s. If multiplied by the SNG exergy flow, it corresponds to 1.79 $/kWh, which is a very high value compared to the cost of the fossil natural gas reported in Table 9. This result is attributable both to the pilot scale of the plant, which entails higher specific costs for the components, and to some pessimistic assumptions made for the economic evaluation. In fact, the lifetime of the plant can be extended to 20 years because the replacements of the SOEC stack (which are expected to take place every 5 years) can be accounted in the O&M cost which is very high. Then, this kind of plant is designed to convert the surplus electricity into a fuel. Therefore, it should be fed with electricity with a very low cost. For this reason, a second set of economic evaluation parameters was tested and they are reported in Table 9.

[6] Π_F thermoeconomic cost of the fuel; $\Pi_P$thermoeconomic cost of the product; Z component cost.

In the new situation, the thermoeconomic cost of the SNG equal to 5.6 c$/s, corresponding to 75 c$/kWh.
The value is still very high, but it is 60 % lower than the previous one, meaning that the plant has to function most of the year in order to recover the quite high fixed cost linked to the construction. For this reason it is advisable to place a storage tank for the electrolyzed gas between the SOEC and the methanation section as describes in section 2. This device would allow the plant not to be constrained by the intermittent production of the electricity, raising the capacity factor. With the economic assumptions of case B the costs of the component and the cost for exergy destruction were computed.
Table 11 is useful to assess the subdivision of the operational costs between those linked to the inefficiencies of the components and those related to the equipment purchase and maintenance. The first step consists in the evaluation of the components with the highest relative variation of the unit thermo-economic cost. Then, the exergoeconomic factor of these components must be analysed. If a component has an exergoeconomic factor close to 1, it could be worth reducing its investment cost (and consequently its efficiency). Conversely, if a component has an exergoeconomic factor close to 0, its efficiency (and consequently its investment cost) could be incremented.

Table 10: Exergetic and thermoeconomic costs for the plant (Case A). For brevity reasons only the main streams are reported

Mass/energy stream	Exergetic cost, E* [kW]	Unit exergetic cost, k_i	Thermoeconomic cost Π [c$/s]	Unit thermoeconomic cost c_i [$/kJ]
Wel pump	0.008	1.000	0.00	1.79E-05
1	0.53	1.000	0.00	4.43E-05
2	0.54	1.004	0.00	4.41E-05
3	4.13	2.870	0.18	1.26E-03
4	18.67	2.404	0.84	1.08E-03
5	21.10	2.218	1.06	1.12E-03
8	163.38	1.000	0.10	6.27E-06
9	165.40	1.003	0.30	1.80E-05
Wel biogas compressor	2.02	1.000	0.00	1.79E-05
10	167.81	1.010	0.38	2.30E-05
11	188.91	1.082	1.45	8.28E-05
16	203.04	1.089	2.18	1.17E-04
17	334.68	1.096	7.20	2.36E-04
Wel SOEC	137.53	1.000	0.25	1.79E-05
18	322.80	1.096	6.95	2.36E-04
19	319.21	1.096	6.87	2.36E-04
20	319.21	1.102	6.87	2.37E-04
21	340.97	1.131	8.96	2.97E-04
Wel methanation compressor	21.76	1.000	0.04	1.79E-05
22	794.11	1.143	22.30	3.21E-04
26	777.17	1.151	22.85	3.38E-04
Wel recirculation compressor	0.19	1.000	0.00	1.79E-05
27	324.21	1.151	9.53	3.38E-04
33	321.43	1.184	13.46	4.96E-04
34	0.36	1.184	0.02	4.96E-04
35	5.89	1.096	0.00	0.00E+00
37	3.63	2.458	0.07	5.05E-04

The components with the highest relative increase in the product cost are the water heaters and the SOEC. The first group is characterized by a very low exergoeconomic factor, while the SOEC has a very high one. This means that the formers should be designed in order to have a higher equipment cost, increasing their exergetic efficiency. Nevertheless, it would be advisable only in the case the surplus heat could find another use. Otherwise it is better to deploy the high exergetic content of the flows to decrease the investment cost. The SOEC is in a different situation because its efficiency is very high and the majority of the increase of the cost is due to the equipment cost. This entails that if there are technical solutions that imply significant cost reductions, they should be considered also in case of decrease in efficiency.

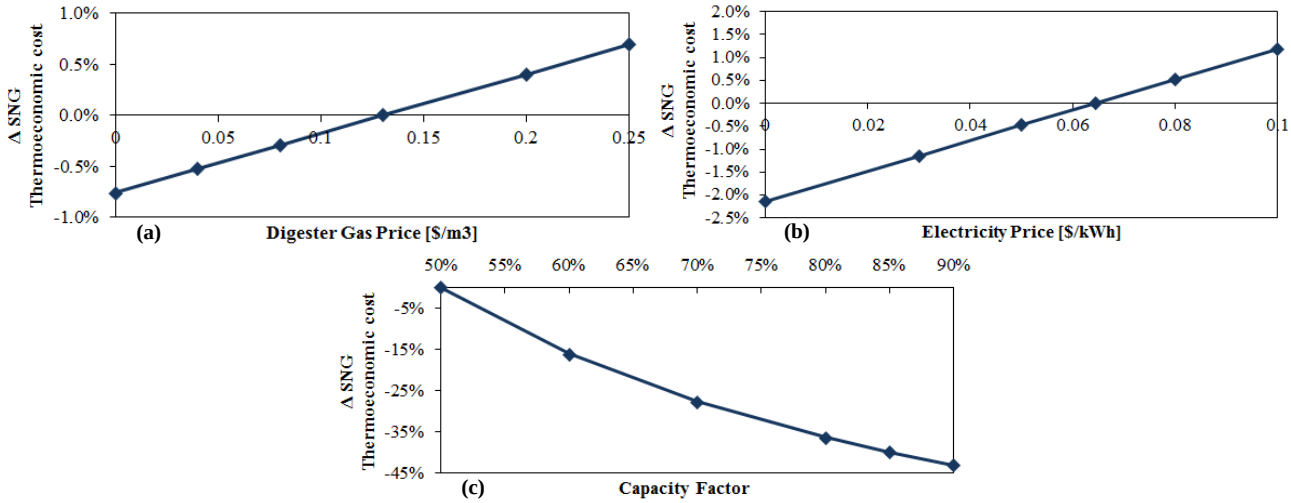

Figure 3: Percentage variation of the SNG thermoeconomic cost versus digester gas price (a), electricity price (b) and capacity factor(c) for case A.

A sensitivity analysis was performed (Figure 3) in order to assess the weight of some assumptions on the thermoeconomic cost of the SNG. It is referred to Case A (Table 9), but the results are similar also for Case B. In particular, the capacity factor is the parameter that affects the variation of the SNG cost to the greatest extent (it is almost halved passing from 50% to 90% of the CF). The prices of the resources influence linearly the cost of the outcome, but their relative weigh is almost negligible compared to the CF. This means that the design of the plant should be based on very reliable estimations on the operating hours of the plant, because otherwise its economic evaluation would be widely compromised.

Table 11: Thermoeconomic performance of the plant under the new economic assumptions

Component	Cost for exergy destruction, C_D [c$/s]	Exergo-economic factor, f_e	Component cost, Z [c$/s]	Fuel cost, c_f [$/kJ]	Product cost, c_p [$/kJ]	Relative difference, r
PUMP	6.561E-04	0.0%	0	2.99E-03	4.15E-03	39%
HE2	2.101E+00	2.0%	4.338E-02	8.85E-03	3.26E-02	268%
HE4	4.879E+00	2.0%	9.718E-02	7.70E-03	1.56E-02	102%
HE5	8.051E-01	7.3%	6.362E-02	2.25E-02	2.75E-02	22%
BIOGAS COMPRESSOR	2.459E-02	76.7%	8.092E-02	5.07E-04	1.19E-03	135%
MIXER 1	1.118E-03	0.0%	0	3.81E-05	3.83E-05	1%
HE3	4.196E+00	0.2%	6.409E-03	4.72E-02	8.20E-02	74%
HE1	3.299E-01	35.4%	1.810E-01	3.29E-03	3.81E-03	16%
HE6	9.696E-03	68.4%	2.103E-02	5.19E-04	6.83E-04	32%
MIXER 2	5.062E-03	0.0%	0.000E+00	5.24E-05	5.24E-05	0%
SOEC	9.354E-02	95.6%	2.028E+00	7.11E-05	2.42E-04	240%
DESULFURATOR	2.867E+00	0.0%	0	1.87E-02	-	-
PRE-METHANATION COMPRESSOR	1.326E+00	39.6%	8.706E-01	1.32E-03	3.20E-03	143%
MIXER 3	7.285E-03	0.0%	0	1.34E-04	1.34E-04	0%
METANATOR 1	4.188E-02	90.4%	3.934E-01	1.34E-04	1.40E-04	5%
RECIRCULATION COMPRESSOR	1.336E+00	0.6%	7.732E-03	2.88E-01	3.80E-01	32%
COOLER 1	9.498E+00	0.6%	5.329E-02	7.05E-02	-	-
SPLITTER 2	0	-	0	-	-	-
METANATOR 2	1.738E-02	95.8%	3.934E-01	1.41E-04	1.56E-04	10%
COOLER 2	4.345E+00	0.4%	1.906E-02	8.69E-02	-	-
METANATOR 3	4.948E-03	98.8%	3.934E-01	1.57E-04	1.71E-04	9%
COOLER 4	4.758E+00	15.9%	9.008E-01	9.72E-03	-	-
DRUM	2.219E-02	0.0%	0	2.07E-04	2.08E-04	0%

10. Conclusions

The thermoeconomic evaluation of the plant showed the strong influence of the size and of the number of operating hours on the economic feasibility of the process. Despite the very high value of exergy efficiency, since the analysis was performed with a pilot-scale plant (~160 kW_{el}) the economic assessment of some equipment costs have been affected by the choice of such a small

scale with a consequent non-linear increase of the cost. Moreover, the hypotheses made on the operation of the plant were very restrictive. Considering a lifetime of the plant of only 10 years, a high interest rate and a low capacity factor has influenced negatively the thermoeconomic performance of the plant. A sensitivity analysis has shown that particular care should be taken in the estimation of the full load hours of the plant, indicating that the economic feasibility could be reached only in case of nearly continuous operation.

In fact, by modifying some operating and financial assumptions the production costs decrease considerably, even though the influence of the size is still very large. For this reason, it is necessary to rescale the plant in order to make it compatible with industrial applications (~1-10 MW). This further analysis could clarify to which extent the technology is mature under the technical and economical perspective.

11. Bibliography

[1] P. Weiland, "Biogas production: current state and perspectives," *Appl. Microbiol. Biotechnol.*, vol. 85, no. 4, pp. 849–60, Jan. 2010.

[2] H. Song, F. Starfelt, L. Daianova, and J. Yan, "Influence of drying process on the biomass-based polygeneration system of bioethanol, power and heat," *Appl. Energy*, vol. 90, no. 1, pp. 32–37, Feb. 2012.

[3] P. Mckendry, "Energy production from biomass (part 2): conversion technologies," vol. 83, no. July 2001, pp. 47–54, 2002.

[4] E. Ryckebosch, M. Drouillon, and H. Vervaeren, "Techniques for transformation of biogas to biomethane," *Biomass and Bioenergy*, vol. 35, no. 5, pp. 1633–1645, May 2011.

[5] "From solid fuels to substitute natural gas (SNG) using TREMP™."

[6] X. Sun, M. Chen, S. H. Jensen, S. D. Ebbesen, C. Graves, and M. Mogensen, "Thermodynamic analysis of synthetic hydrocarbon fuel production in pressurized solid oxide electrolysis cells," *Int. J. Hydrogen Energy*, vol. 37, no. 22, pp. 17101–17110, Nov. 2012.

[7] J. B. Hansen, "Process for converting biogas to a gas rich in methane," WO2012003849 A1, 2012.

[8] F. Petipas, Q. Fu, A. Brisse, and C. Bouallou, "Transient operation of a solid oxide electrolysis cell," *Int. J. Hydrogen Energy*, vol. 38, no. 7, pp. 2957–2964, Mar. 2013.

[9] J. Udagawa, P. Aguiar, and N. P. Brandon, "Hydrogen production through steam electrolysis: Model-based dynamic behaviour of a cathode-supported intermediate temperature solid oxide electrolysis cell," *J. Power Sources*, vol. 180, no. 1, pp. 46–55, May 2008.

[10] D. Ferrero, A. Lanzini, M. Santarelli, and P. Leone, "A comparative assessment on hydrogen production from low- and high-temperature electrolysis," *Int. J. Hydrogen Energy*, vol. 38, no. 9, pp. 3523–3536, Mar. 2013.

[11] I. Kemp, *Pinch Analysis and Process Integration*, 2nd ed. Oxford, 2007.

[12] "Aspen Physical Property System (Physical Property Methods)," 2010.

[13] H. N. Moran, Michael J, Shapiro, *Fundamentals of Engineering Thermodynamics*, 5th ed. John Wiley & Sons, Inc, 2006.

[14] R. Turton, *Analysis, Synthesis and Design of Chemical Processes*, Third Edit. Prentice Hall.

[15] L. Rath, "Cost and Performance Baseline for Fossil Energy Plants Volume 2 : Coal to Synthetic Natural Gas and Ammonia," 2011.

[16] M. Marsh, C. E. Officer, K. Krich, D. Augenstein, J. Benemann, B. Rutledge, and D. Salour, "Biomethane from Dairy Waste - A Sourcebook for the Production and Use of Renewable Natural Gas in California," 2005.

[17] M. Gandiglio, a. Lanzini, P. Leone, M. Santarelli, and R. Borchiellini, "Thermoeconomic analysis of large solid oxide fuel cell plants: Atmospheric vs. pressurized performance," *Energy*, vol. 55, pp. 142–155, Jun. 2013.

[18] A. Valero, M. Lozano, and M. Munoz, "A general theory of exergy saving, parts I, II and III," *Comput. Eng. Energy Syst.*, vol. 3, pp. 1–22, 1986.

[19] F. R. Szargut, J., Morris, D. R., and Steward, *Energy Analysis of Thermal, Chemical, and Metallurgical Processes*. New York: Hemisphere, 1988.